

The authors dedicate this paper to the memory of the prominent geologist Professor Radu Dimitrescu, PhD, Doc., who initiated us into the study of microtectonics, inviting us for a few days, in 1963, to perform common studies at Arieșeni and Avram Iancu (Apuseni Mountains)

THE Na-MONTMORILLONITIC AND Na-BEIDELLITIC BENTONITE FROM VALEA CHIOARULUI (MARAMUREȘ COUNTY, ROMANIA)

LUCREȚIA GHERGARI, IOAN MÂRZA

Department of Mineralogy, Faculty of Biology and Geology, “Babeș-Bolyai” University Cluj-Napoca, Str. M. Kogălniceanu, nr. 1. E-mail: lucretia.ghergari@ubbluj.ro; marza.ioan@gmail.com

Abstract. The genesis of the bentonite ore from Valea Chioarului (Maramureș County, Romania) is related to volcanic rocks, *i.e.*, vitrophyric rhyolite and porous vitroclastic tuff that crop out on a very limited surface: 450 m in length and no more than 40–50 m in thickness. From a morphological-structural point of view, the ore can be defined as “diatreme” or “breccia dyke” with N–S orientation resulted during a phreatic explosion. Associated to the rhyolitic volcanism, a two-phase hydrothermal mineralization was identified: a higher temperature phase (280°–320° C) represented by quartz and amethyst in geodes (up to 50×20 cm in size), and a lower temperature represented by microcrystalline quartz, moganite, cristobalite, opal, celestine, and barite. This paper focuses on the study of the argillization process by using complex analytical methods: mineralogical and chemical analyses, TEM and SEM, X-ray diffraction and IR spectroscopy. Both volcanic rocks underwent a hydrothermal transformation in the argillitic, *i.e.*, bentonitic stage, mainly associated to the second mineralogenetic phase. This process was controlled by epithermal fluids, with the contribution of sea water thermalized during the phreatomagmatic stage. The argillization intensity was heterogeneous, locally reaching up to 90 %. The main clay minerals are Na-montmorillonite and Na-beidellite; halloysite occurs subordinately and kaolinite, illite, illite/montmorillonite and micas, accidentally. The excess of SiO₂ resulted in the argillization process *i.e.*, cristobalite, was concentrated as silica nodules in the bentonite mass. The main source for Na (0.75 %) was the protolith submitted to bentonitization, enriched via the hydrothermal fluids supply, including the thermalized sea water.

Key words: bentonite, Na-montmorillonite, Na-beidellite, Valea Chioarului, Romania.

Résumé. Le gisement de bentonite de Valea Chioarului (département de Maramureș, Roumanie) a été formé suite à l'effet auto-hydrothermal d'un corps volcanique (rhyolite vitrophyrique et tuf vitroclastique poreux) de petites dimensions (450/40–50 m) de type dyke de brèche orienté nord-sud. Le corps volcanique, appartenant au magmatisme laramique, est le résultat d'une explosion phréatique localisée au contact tectonique entre formations sédimentaires détritiques sénoniennes et paléogènes. Il y a deux phases de minéralisation hydrothermales associées au volcanisme: une première phase de haute température (320–280°C) représentée par quartz et améthyste (géodes de 50×20 cm, dans la zone centrale), suivie par une phase majeure généralisée, de basse température (quartz microcristalline, moganite, cristobalite, opale, célestin et barytine), contemporaine à la métasomatose de la roche volcanique – volcano-hydroclastique, responsable de la forte argilisation de la roche dans une proportion d'environ 90% (localement il existe des zones non-altérées soit faiblement affectées). À part d'une présentation synthétique de la géologie de la région liée au volcanisme et l'altération hydrothermale, notre étude insiste sur le processus d'argilisation – bentonitisation en se basant sur une série complexe de méthodes d'analyses: minéralogiques, chimiques, MET et MEB, diffraction rayons X, spectrométrie IR. Les minéraux identifiés sont les suivants: Na-montmorillonite, Na-beidellite, principalement; halloysite, subordonné; kaolinite, illite, illite/montmorillonite et micas rarement. L'excès de silice apparut suite à l'argilisation s'est concentré sous forme de nodules (cristobalite, quartz microcristalline) de petites dimensions, dispersés d'une manière aléatoire dans la masse argilisée. La source principale du Na (0.75 %) a été la roche volcanique bentonitisée – élément enrichie dans les fluides hydrothermaux –, et partiellement par apport de l'eau marin (phréatique). L'occurrence de Valea Chioarului représente la plus importante masse de Na-bentonite de Roumanie.

Mots-clés: bentonite, Na-montmorillonite, Na-beidellite, Valea Chioarului, Roumanie.

1. INTRODUCTION

The bentonite ore from Valea Chioarului (Maramureș County) represents the largest accumulation of Na-montmorillonite and Na-beidellite from Romania. Its special features, such as ionic exchange, adsorption and expandability – all reversible properties during a large number of cycles under suitable technical parameters, turn this bentonite into a raw material of interest for several industrial applications.

Hauer and Stache provided the first geological data on Valea Chioarului area (Hauer, Stache, 1863); more detailed investigations were performed by Hofmann (1880), who defined the primary rock as “rhyolite–dacite”. Grengg studied in detail (Grengg, 1920, (Grengg, 1940) the local bentonite (*i.e.*, from “Gaura”, the former name of Valea Chioarului locality), which he called “soapy earth” (in German: seifige Erde). In his view, the bentonite resulted by a deep-rooted disaggregation–alteration process affecting a vitrophyric “liparite”. Subsequently, Szentés considered that the primary rock was represented by a rhyolitic tuff (Szentés, 1950).

Detailed studies on Valea Chioarului bentonite and on the regional geology were published in the second half of the 20th century. Based on similarities with the situation described by Cloos from Germany (Cloos, 1969), in 1953 Chiriac¹ envisioned the existence of an explosion vent generating the rhyolitic–dacitic tuffs that represented the primary rock for the bentonitization process. Noveanu (1960, unpublished)² considered volcanic ash deposited in a marine environment as the originary rock. Mârza and Ghergari started the series of modern studies on the mineralogy of the bentonite by using electron microscopy, thermal analysis and X-ray diffraction; based on these analyses, and on the regional geological features, the authors suggested a hydrothermal genesis for the bentonite (Mârza, Ghergari, 1963, 1967). Ioniță introduced additional features in the presentation of the geology of the region, such as the presence of Bârsăului Valley fault (Ioniță, 1964). He also defined the primary rock of the bentonite as rhyolite–dacite. Mărgărit and Mărgărit focused on the stratigraphy of the Paleogene deposits in Valea Chioarului area (Mărgărit, Mărgărit, 1968).

Kalmár and Ionescu provided remarkable details by characterizing the regional geology (sedimentary rocks and their succession), and the petrochemistry and mineralogy of the bentonitic rocks (Kalmár, Ionescu, 1972), (Kalmár, 1975). These authors favoured the idea of a phreatic explosion; also, they have associated the volcanic rock to the banatites. Based on recent data on the age of the bentonitized volcanic rock, Ștefan and his co-authors assigned the “vitreous rhyolite” to the banatitic stage, as northern extreme occurrence in the Apuseni Mountains–Moigrad–Valea Chioarului alignment (Ștefan *et al.*, 1986), (Ștefan *et al.*, 1988). Onac (1987) presents a general geological overview of the Valea Chioarului region in his graduation paper³. Ghiurcă and Mârza have characterized the Badenian deposits within Valea Chioarului ore, focusing on the volcanic (fall-out) tuffs (Ghiurcă, Mârza, 1991). A study of (hydrothermal) gem-quality minerals in the bentonite was performed by Ghergari and Ionescu (Ghergari, Ionescu, 2000).

2. GEOLOGY OF THE REGION – THE BENTONITE ORE

There is no known surface occurrence of the crystalline basement in the Valea Chioarului area. Nevertheless, blocks of ~ 1m in size of micaschists with staurolite and almandine were noticed along Runcului Valley (a left tributary of Bârsăului Valley); these rocks are compatible with the mezometamorphic facies of the Baia de Arieș Series, in the Apuseni Mountains.

¹ Chiriac, M., 1953, *Geological report, The Bentonite Ore from Valea Chioarului, Baia Mare Region* (in Romanian: *Zăcămintul de bentonit de la Valea Chioarului, regiunea Baia Mare*. Raport geologic), Archive of the Geology and Geophysics Institute, Bucharest.

² Noveanu, I., 1960. *Geological-mining report, Valea Chioarului, 1960*, Cluj, “Cominex” Archive, Cluj-Napoca.

³ Onac, B. P., 1987, *Geological, stratigraphical and paleontological study of the geological formations from the Mesteacă – Vărai – Valea Chioarului region* (in Romanian: *Studiul geologic, stratigrafic și paleontologic al formațiunilor geologice din perimetrul Mesteacă – Vărai – Valea Chioarului*, lucrare de diplomă, 85p), Babeș-Bolyai University, Geological Library.

The sedimentary deposits consist of: Cretaceous (Coniacian–Santonian) flyschoid purplish interlayered marls and siltites with inoceramus, echinids and ammonites (in Dâmbul Morii Hill, Untului Brook, or Bârsăului Valley); Paleogene variegated, ferruginous clays and gravel complex (Popescu, 1978), (Popescu, 1984); Upper Eocene limestones; Oligocene marls; and Badenian marls with volcanic tuffs interlayers displaying paleontological features typical for the Leitha Facies (Fig. 1a, b).

Within the outcrop, the *eruptive* body – consisting of both bentonite and fresh primary rocks – is enrooted in the Jibou Formation (Paleogene), meters away from the contact with the Cretaceous sediments. The intrusion was emplaced along a tectonic line, and the contact is visible in outcrops, from the left bank of Untului Brook in the North, to the Lucățel Brook or Olăriței Valley in the South. We interpreted this isolated magmatic body as an apophysis of a deeper acidic intrusion that evolved into a phreatomagmatic structure towards the surface.

Concerning the ore body morphology, Chiriac⁴ considered it as an *explosion vent*, Mârza and Ghergari – a *dyke* (Mârza, Ghergari, 1967), while Kalmár – an *extrusion neck* (Kalmár, 1975). Based on hard evidences, if one accepts the explosive origin – thus the contribution of tuffaceous material, the more appropriate term would be *diatreme* or “*breccia dyke*” (phreatic explosion). Along its maximum, north–south extension, the bentonitized body is 40–50 m in length, with a N30°W/40°SW orientation. The base and top contacts of the ore with its neighbouring sedimentary deposits are sharp.

3. SAMPLES AND METHODS

The complex mineralogical–petrographical study of the Valea Chioarului bentonite ore was performed on 40 samples collected from underground works and surface outcrops. Table 1 summarizes data on the rock type, sample location and a brief macroscopic description of these samples.

The sample preparation consisted in grain-size separation. The bentonite sample was mixed with distilled water in a centrifuge cell for 10–20 minutes. The suspension of clay and water was poured over a 0.063 mm mash sieve and the remaining solution was recovered. This procedure was repeated until all the <0.063 mm grains passed through the sieve. The material left on the sieve, *i.e.*, the residue (R) – representing the arenite and rudite classes, was dried and weighted. The dry suspension, corresponding to the levigated fraction (PL), consisted of lutite and silt grains. Two of the levigated samples were used for further separating the clay fractions <5 μm and respectively <2 μm. We have quantitatively separated these clay fractions by using the sedimentation–siphoning method until the clay + water solution remained clear.

This separation method is based on the principle of free settling of solid particles in fluids based on their own weight, as expressed by Stokes' law:

$$v=2/9g*r^2(\gamma_m-\gamma_l/\eta) \quad (1)$$

where: v is the particles' settling velocity in liquid (cm/sec); g – the gravitational acceleration; r – the particle's radius; γ_m – the particles' mass density [of the]; γ_l – the fluid mass density; η – the liquid's viscosity coefficient.

From the two clay fractions, we have prepared oriented samples for the X-ray diffraction investigation; from the < 2 μm fraction, we have also prepared parlodion-carbon pellicles for the transmission electron microscopy (TEM) study.

⁴ Chiriac, M., 1953, *Geological report, The Bentonite Ore from Valea Chioarului, Baia Mare Region* (in Romanian: *Zăcămintul de bentonit de la Valea Chioarului, regiunea Baia Mare*. Raport geologic), Archive of the Geology and Geophysics Institute, Bucharest.

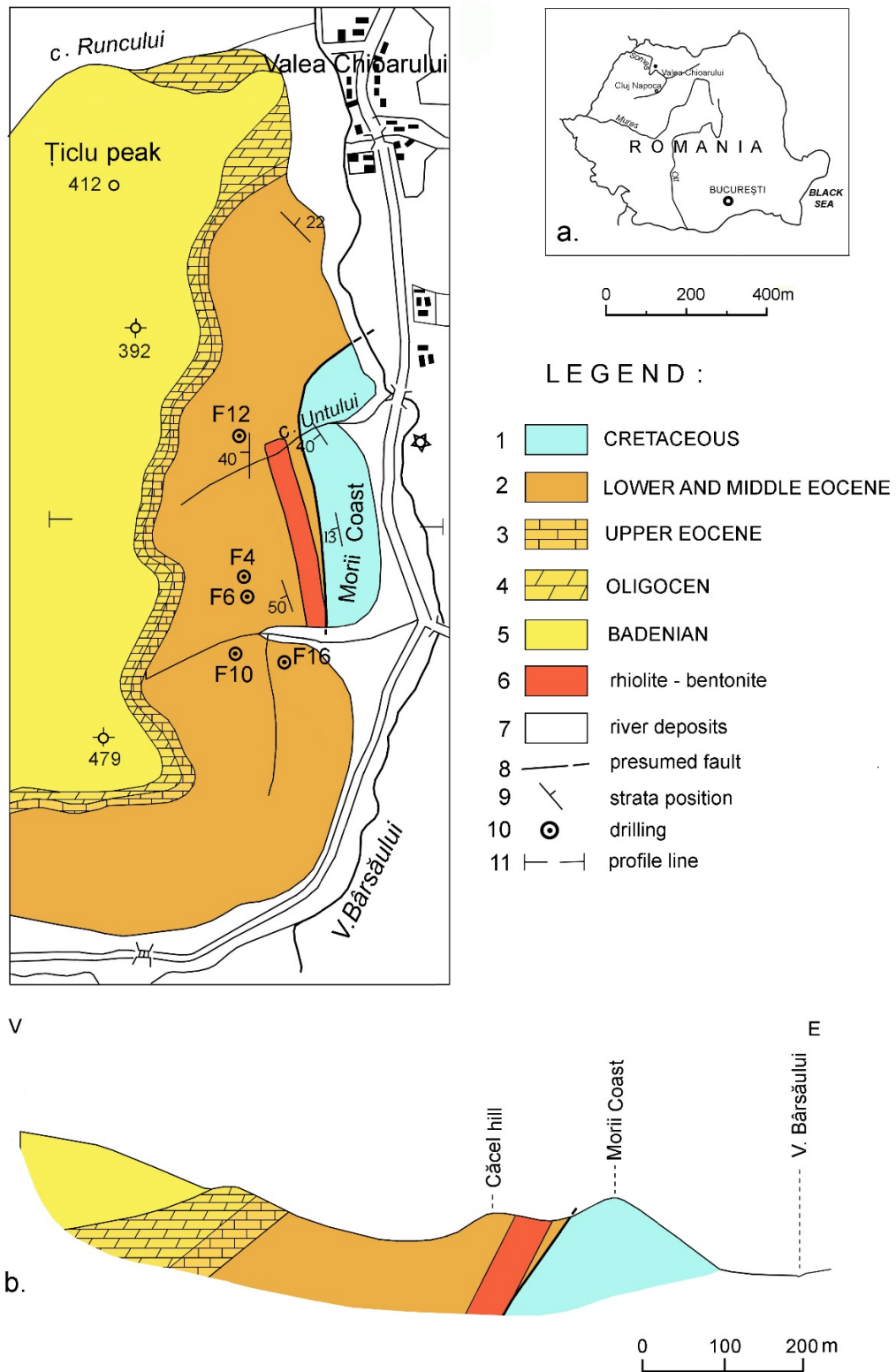


Fig. 1 – Geological map of the Valea Chioarului bentonite ore (Mârza & Ghergari, 1967).
 a) Location of the Valea Chioarului area on the map of Romania; b) Geologic cross section through the ore.

Table 1

Geological data on the studied samples

Sample no.	Rock type	Location	Macroscopic features (\emptyset =diameter)
<i>Underground samples</i>			
1	Bentonite: greyish, greyish–reddish	Panel 12B, slice 11 (3 m from the clays in the hanging wall)	The rock preserves fresh crystal fragments of feldspars, quartz and only partly altered biotite
2	Bentonite: light greyish, compact	Panel 12B, slice 11 (right-hand mine chamber)	The rock contains numerous sedimentary elements (3–4 cm \emptyset) from the neighbouring area, mainly consisting of rounded quartzite clasts and sandy clay
4	Bentonite: white with greenish spots, compact	Panel 10A, slice 12 (18–20 m from the bedrock)	The rock contains numerous crystals and fragments of feldspars, chloritized biotite and rare sedimentary elements
5	Bentonite: white, when dry	Panel 10A, slice 12 (~50 cm from the contact, orientation 45°/SW)	The rock contains fragments of micaceous sandstone (Cretaceous), frequent feldspar relics, quartz, and intensely chloritized feldspars; the bentonite is partly silicified
7	Bentonite: greyish, compact	Panel 9, slice 13	The rock contains relic crystals of feldspars, quartz, partly chloritized biotite, and rounded metamorphic clasts (1–2 mm \emptyset).
8	Bentonite: greyish, hard (incomplete argillization)	Panel 9, slice 13 (10 m from the mining front)	The rock contains plagioclase, quartz, and chloritized biotite crystalloclasts, and accidentally small (2–3 mm \emptyset) fragments from the sedimentary host-rock and silica micronodules (1–3 mm \emptyset) in the residue
13	Bentonite: greyish–slightly greenish, intensely breccified	Panel 4, slices 1–5 (bedrock, close to the limit with the Cretaceous deposits)	The rock contains crystalloclasts of quartz, feldspar and relatively fresh biotite lamellae; silica nodules (1–3 cm \emptyset) are also present
14	Bentonite: grey–greenish with silica (“quartzine”, cristobalite) nodules	Panel 4, slice 15	The rock contains significant amounts of partly chloritized biotite, rare feldspar crystals and rounded quartzite fragments (up to 2cm \emptyset) from the sedimentary host rocks. The silica nodules (1–4 cm \emptyset) represent ~25 % of the bentonite mass; they display an irregular shape, rough surface, and contain celestine and barite partly replaced by silica
23	Bentonite: light greyish, compact	Panel 12B, slice 12 (hanging wall, preparation shaft, at ~3 m from the contact with the variegated horizon)	The rock contains sedimentary elements (3–4 cm \emptyset), quartzite fragments – mainly rounded – and sandy clay
15–21	“Amethyst” (quartz variety) crystals in geodes; opal-C crust; “chalcedony”; “quartzine”; barite and Celestine, partly replaced by “chalcedony”; halloysite associated with cristobalite; moganite.		
<i>Surface samples</i>			
24–25	Rhyolite: massive, greyish (pechstein-type)	Porphyric fabric with glassy groundmass	
26–27	Vitrophyric tuff: reddish–brownish	Porphyric fabric with sphaerolitic groundmass	
28–29	Vitroclastic tuff: greyish, grey–reddish	Vitroclastic fabric	
30–31	Vitroclastic tuff: porous, white	Porous vitroclastic fabric	
32–33	Andesite	Porphyric fabric with microcrystalline or glassy groundmass	
34–35	Marls and sandstones	Coniacian	
36–38	Sands, gravels	Paleogene	
39–40	Sandy clays: red	Paleogene	

The analytical methods used for this study were: optical microscopy in transmitted polarised light on Jenapol and Nikon Optiphot 2/Pol microscopes with Nikon FDX-35 photo camera – on thin sections, transmission electron microscopy (TEM) on a Tesla B650 unit, and scanning electron microscopy (SEM) on a Tesla unit (the sample being covered with a gold pellicle), IR spectroscopy (on pellets made of a mixture of KBr with 0.125 % clay fraction), and X-ray diffraction (XRD) on raw and oriented (treated with ethylene glycol, or heated) samples on a Dron 3 unit. The experimental parameters for the diffractometric work were: 20 kV voltage, 20 mA intensity, 2°/minute scan speed on the 2°–64° 2 θ interval, monochromatic radiation ($\lambda_{\text{K}\alpha}=1.54051 \text{ \AA}$), Cu anticathode and Ni filter.

4. RESULTS

4.1. PETROGRAPHY OF THE BENTONITIZED VOLCANIC ROCK

In spite of its limited volume, the bentonitized rock from Valea Chioarului displays impressive structural–textural and chromatic complexity; some of these varieties were identified only as fragments, along Untului Valley. Although at geological scale it appears as a trivial item, this body has raised at least three challenging issues: *the nature of the protolith* affected by bentonitization, the path and *source of the argillization*, and the *geological age*, *i.e.*, the assignment to a tectonic-magmatic cycle. Some of the peculiar aspects that render answering these questions difficult, are: this body is an isolated geological feature as compared to both the banatitic province – located south–westwards, and to the Neogene volcanics province, located northwards; the structural–textural diversity of the fresh rhyolite, and the lack of clear relationships between the various bentonite varieties present as fragments distinguishable *in situ* (Untului Brook).

The study of a systematically collected set of underground (from the slightly bentonitized rock, the core rock and the bentonite proper), and surface samples revealed the existence of the following petrographic varieties and peculiar features:

Massive, greyish vitrophyric rhyolite (pechstein-type) (Figs. 2, 3) with glassy appearance; within the glassy matrix fresh biotite, feldspars and quartz phenoclasts are macroscopically visible.

Under the microscope, we noticed a homogenous, colourless and isotropic glassy matrix (65 %) rich in crystallites–globules (0.02 mm \varnothing), spiculites and margarites (0.004 \times 0.050 mm), anisotropic skeletal crystals (Fig. 4). The common orientation of the prismatic crystallites outlines the rock's fluidal texture. The relative mineral abundance is: quartz 10%, sanidine 14.2%, acidic plagioclase 9 %, biotite 1.5 %, magnetite 0.3 %. Qualitatively, we can mention the high degree of idiomorphism and lack of alteration, the skeletal shape of quartz and some feldspar crystals due to intense magmatic resorption processes.

Quartz is present as isolated or twinned bipyramidal crystals (0.15–1.5 mm \varnothing) with numerous biphasic liquid–gas inclusions; parallel fissures extending into the glassy matrix are very frequent. The sanidine crystals (0.25 \times 0.40 mm up to 1.0 \times 2.0 mm in size) are fresh; if they show twins, they are of Carlsbad type. Based on inclusions, two generations of sanidine with different optical orientations were defined: sanidine I – microlitic, included in sanidine II – phaneritic. Plagioclases (0.25 \times 0.30 mm–1.3 \times 2.2 mm in size) are also fresh; they show polysynthetic twinning and sometimes are included in sanidine crystals. Biotite (0.10 \times 0.25 mm–0.40 \times 0.80 mm in size) displays intense dark to yellowish pleochroism. It is present as phaneritic and microlitic crystals, or it may be included in feldspars. The rims of the biotite crystals expose features of magmatic resorption. Accessory minerals are rare, and they are represented by allanite (0.15 \times 0.30 mm), zircon (0.05 \times 0.08 mm) and apatite (0.015 \times 0.04 mm), the last ones being often present as inclusions in biotite. The succession of magma crystallization was: zircon–allanite, apatite, magnetite (as accessory minerals) biotite, plagioclases, sanidine (I, II), and quartz.

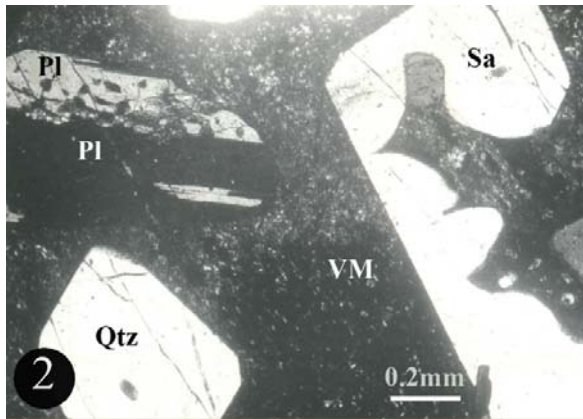


Fig. 2 – Pechstein-type vitrophyric rhyolite. Magmatically corroded sanidine (Sa), plagioclase (Pl), quartz (Qtz) in a glassy groundmass (VM). 1N.

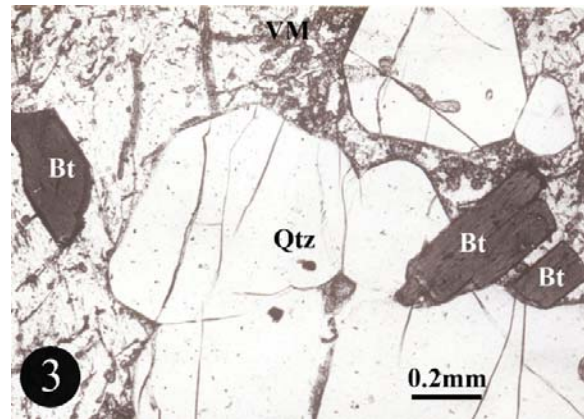


Fig. 3 – Pechstein-type vitrophyric rhyolite. Quartz (Qtz), biotite (Bt) in a glassy groundmass (VM). 1N.

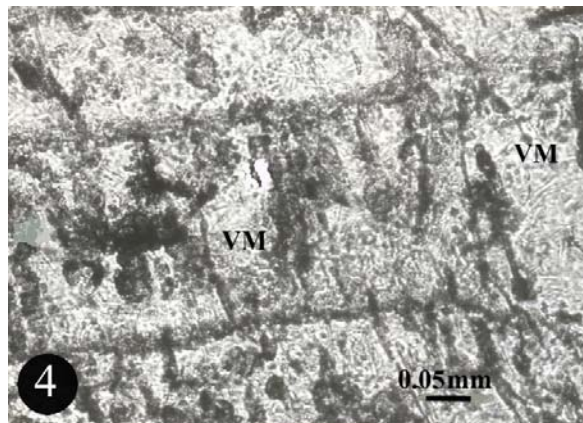


Fig. 4 – The groundmass of the vitrophyric rhyolite. Crystallites in a glassy groundmass (VM). 1N.

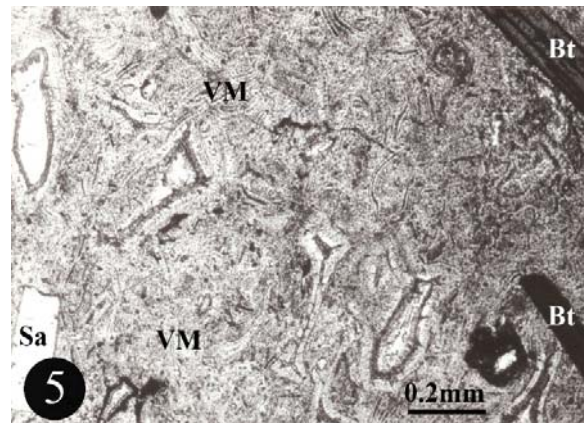


Fig. 5 – Vitrophyric rhyolite. Oriented sanidine (Sa) and biotite (Bt) in a glassy groundmass (VM). 1N.

Reddish-brownish (sometimes randomly spotted) **vitrophyric rhyolite** (Fig. 5) with macroscopically visible biotite, feldspars and quartz. Both rhyolite types occur as fragments, up to 20–30 cm in size, along Untului Brook. In spite of its obvious genetic consanguinity with the bentonitized rock, no direct relationship could be noticed *in situ*. Small enclaves consisting of fragments of Cretaceous and Paleogene sandstones, 2–4 cm in size, are frequent. They are surrounded by a whitish, poorly bentonitized contact aureole. Small (mm- or cm-in size), partly bentonitized nests were identified also in the “fresh rock” matrix.

Microscopically, we noticed sphaerolitic–subsphaerolitic textures in the volcanic glass; the latter was intensely recrystallized and partly replaced by cristobalite. Magmatic minerals are present in small amounts, the glass: crystal ratios varying between 7:3 and 1:9. Quartz and feldspars (sanidine, plagioclases) are intensely corroded *via* magmatic resorption. Biotite shows opaque areas and sometimes magmatically corroded rims. Glass has protruded within the lamellae building-up the biotite aggregates. Both quartzite microxenoliths (0.20 × 0.40 mm in size) – also showing magmatic corrosion features (0.15 mm), and exogenous quartz with undulatory extinction occur seldom in this rock, besides exfoliated biotite. Lithophyses within the rock are bordered by cristobalite, and in some cases are filled with microcrystalline quartz. To summarize, crystalline phases are subordinate components when compared with glass (Table 2).

Table 2

Modal composition of the vitrophyric rhyolite

Component	%	Maximum sizes (mm)
Glass	80	
K-feldspar	6.2	0.8 × 1.2
Plagioclase feldspar	3.4	1.5 × 2.0
Quartz	5.8	0.4 × 0.6
Biotite	4.6	0.7 × 0.8

Vitroclastic tuffs, *i.e.*, the tuffogeneous rocks represent the dominant petrographic variety building-up the geological body under study, both in outcrops (Untului Brook) and in the underground. The partly bentonitized “core” represents the primary rock, or the protolith; it can be identified based on specific structural–textural features preserved also following the argillization process. There are two varieties: grey–greyish–reddish quasi-compact and white porous vitroclastic tuffs – the latter being characteristic for the outcrop in the left bank of Untului Brook.

Grey–greyish–reddish quasi-compact vitroclastic tuffs (Figs. 6, 7).

The microscopical investigation evidenced the presence of volcanic glass fragments ($<0.30 \times 1.20$ mm) displaying X-shaped, Y-shaped, triangular, spherulitic–vesicular, or irregular morphologies. They are colourless and isotropic, and are embedded in a fine, partly recrystallized glassy matrix. The matrix also contains seldom angular quartz fragments (0.50 mm Ø), or sanidine and plagioclases (0.30×0.60 mm) with fresh surfaces; all display clear features of magmatic corrosion. Rare opaque minerals, such as magnetite or pyrite, as well as biotite were also noticed. The glass: volcanic crystalloclasts ratio is ~ 9:1. The rock also contains pumice fragments (0.80×3.50 mm), and fibrous glass with or without feldspar microlites.

The pumice and the fibrous glass are lens-shaped (3×1 cm) and represent the first rock components to be transformed during the bentonitization process. Macroscopically, we have noticed the alteration of irregular obsidian fragments (<1 mm). The rock is highly porous, in both its homogenous and the brecciated varieties. Microscopically, the angular mineral fragments (quartz, feldspars) expose incipient magmatic corrosion features. The vitroclastic tuffs contain frequent xenoliths and xenocrystals (sericitic quartzites in Fig. 8, quartz with undulatory extinction, muscovite, or exfoliated biotite) having as source the Cretaceous and Paleogene country rocks. Fibro-radial “quartzine” was deposited in the voids of the rock, as a secondary phase (Fig. 9).

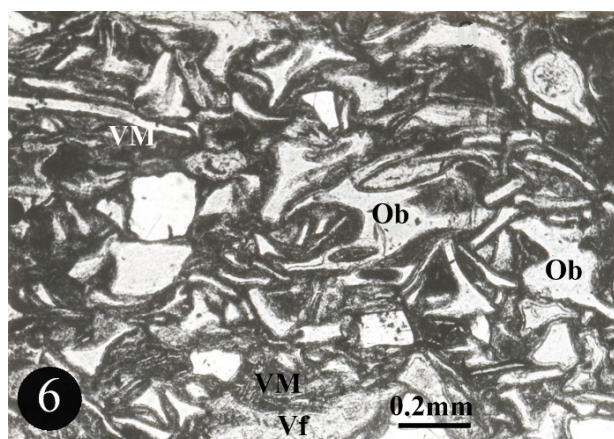


Fig. 6 – Vitroclastic tuff; slightly bentonitized core. Vitroclasts (obsidian – Ob) and micropumice (Vf) in a poorly recrystallized glassy groundmass (VM). 1N.

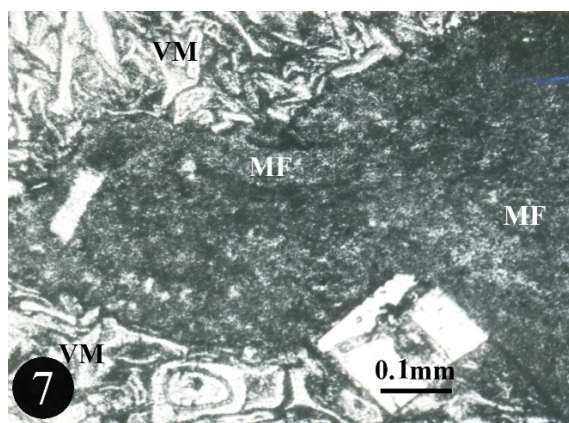


Fig. 7 – Vitroclastic tuff: slightly bentonitized core embedding a rhyolite fragment; poorly recrystallized groundmass (MF). 1N.

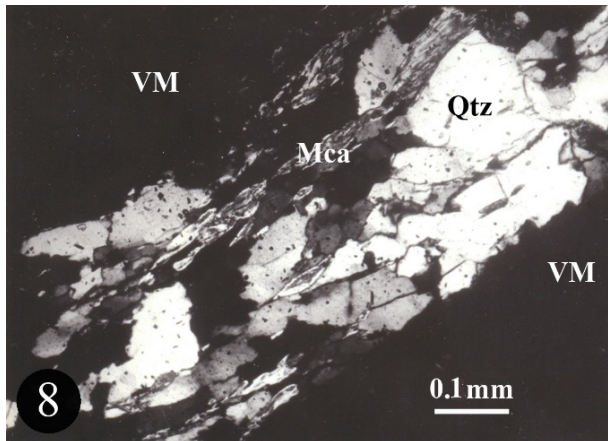


Fig. 8 – Enclave of sericitic quartz in vitroclastic tuff (sample from the underground). N+.

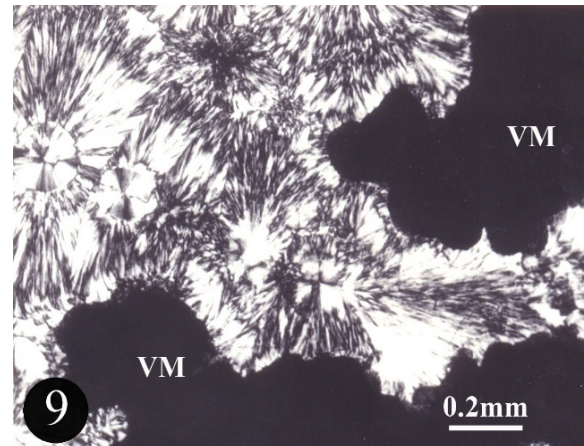


Fig. 9 – Fibro-radial quartz (“quartzine”) formed in the voids of the vitroclastic tuff. N+.

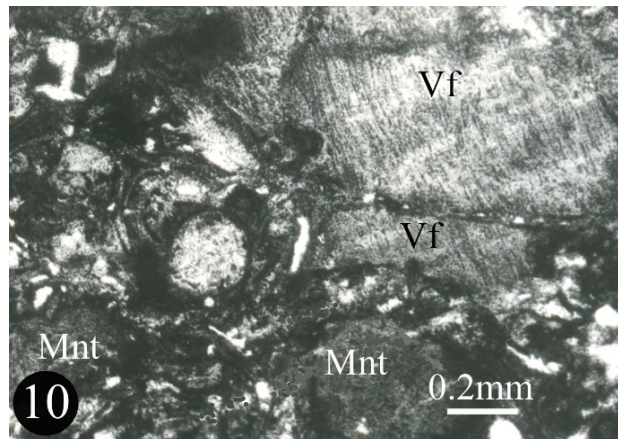


Fig. 10 – Bentonite with fibrous vitroclasts (Vf). Montmorillonite (Mnt). N+

The partly bentonitized central “core” identified in the underground works corresponds to a volcanic tuff. It consists of volcanic glass fragments with typical morphologies, as presented above, embedded in a fine, partly recrystallized glassy matrix. Biotite lamellae that partly lost their idiomorphic outline, as well as flaky quartz grains and feldspars – rarely present as intact crystals, were also evidenced. Additionally, we have also noticed partly recrystallized fibrous vitroclasts with slight signs of magmatic corrosion (Fig. 10).

Bentonitization affected this rock only locally, in nests of 2–3 cm in size, mainly by transforming the pumice fragments and the fibrous vitroclasts thus creating an overall breccious aspect. The levigation of the clay minerals from these nests generates a secondary, vacuolar texture. The fresh rock is dark grey in colour and consists of volcanic glass fragments (frequent obsidian, <1 mm in size), quartz, feldspars, suboriented biotite lamellae and numerous microenclaves of sedimentary rocks (<2 cm in size).

White porous vitroclastic tuffs

The white vitroclastic tuffs are porous and apparently homogeneous rocks. They were partly transformed *via* argillization, silicification, various degrees of Fe-depletion in biotite, or biotite transformation into chlorite. Seldom, the rock contains angular fragments of quartz, feldspars and

sedimentary materials as enclaves. This rock variety represents the typical material in the outcrop from Untului Brook.

Under the microscope, we noticed a glassy matrix with globular texture with rods, triangular shapes *etc.* (where cristobalite might have been deposited), overprinting an inherited vitroclastic structure. Cristobalite forms fibro–radial aggregates (0.03–0.15 mm Ø) that may be surrounded by a circular rim of the same composition (0.007–0.015 mm-thick) (Tab. 5). The glass: crystals ratio is ~9:1, the angular crystals being represented by quartz (0.30 × 0.65 mm–1.10 × 1.60 mm), sanidine (0.60 × 2.5 mm), rarely plagioclase and Fe-depleted, or chloritized biotite.

Under high magnification, the glass attests the presence of pumice vitroclasts (0.80 × 3.50 mm) resulted from a melt rich in gases. Its recrystallisation and the formation of cristobalite cause the hyaline paste to get restructured, with the formation of triangular, simple or concentric–overlapping elliptic–spheroidal, half–moon, or irregular lithophyses, bordered by/filled with cristobalite and clay minerals. The planimetric investigation evidenced the following modal mineralogical composition: 80–90 % glass, 10–20 % angular crystals represented by quartz (4–8 %), sanidine (2–5 %), acidic plagioclase (3–4 %), and biotite (1–3 %). In one thin section we have identified a magnesiohornblende crystal (0.02 × 0.04 mm); accidentally, microlites of zircon and opaque minerals were also noticed.

Table 3

Mineral assemblage based on the whole rock XRD pattern (sample 7)

XRD parameters		Assignment of the corresponding lines			
<i>d</i>	<i>I</i>	<i>Crs</i>	<i>Fsp</i>	<i>Chl</i>	<i>Mnt</i>
14.335	2			+	
12.911	2				+
7.132	4			+	
6.505	3		+		
5.854	3				
4.736	2			+	
4.448	7				+
4.206	20		+		
4.036	100	+			
3.766	16		+		
3.572	4			+	
3.450	10		+		
3.275	18		+		
3.213	20		+		
3.131	6	+			
2.985	12		+		
2.896	6		+		
2.837	10	+			
2.760	5		+	+	
2.572	8		+	+	
2.481	20	+			+

Legend: Crs=cristobalite, Fsp=feldspar, Chl=chlorite, Mnt=Montmorillonite

The hydrothermal minerals association

The presence of hydrothermal (non-clay) minerals in the Valea Chioarului bentonitic ore deposit pleads for the circulation of postmagmatic solutions, genetically related to the bentonite's petrogenesis. Two stages of hydrothermal mineralisations can be separated:

– ***a high temperature stage***, probably preceding the bentonitization, defined by the formation of quartz – amethyst variety, in geodes;

– ***a low temperature stage*** (typical epithermal) that is responsible for the argillization process. Besides clay minerals, other low temperature minerals formed: microcrystalline quartz, moganite, cristobalite, opal, celestine and barite – the last two minerals being first time identified at Valea

Chioarului by the geologist V. Todoran, who has identified geodes up to 50 cm in length and 20 cm in width in the bentonite mass (panel 15, slice 10 and panel 5, slice 9). The outer crust of these geodes consists of a compact microcrystalline aggregate of pink-bluish moganite (Ghargari, Ionescu, 2000), while the inner space is lined with amethyst crystals (up to 1 cm in length) sprinkled with hematite spherules and marcasite microcrystals. Mineral geothermometry data on amethyst⁵, and on oriented biphasic liquid–gas inclusions plead for a homogenisation temperature of 280°–320° C.

The silica nodules, millimetre to 10–20 cm in size, are sometimes present in large amounts in the bentonite (e.g., panel 4, slice 1–5); their formation is related to the segregation/accretion of excess silica resulted during the argillization process. Mârza and Ghargari have identified halloysite associated with cristobalite, along less than 5 cm thick fissures–fractures (Mârza, Ghargari, 1967).

5. BENTONITIZATION

Hydrothermal fluids rich in water and gases, with low silica but significant sodium content and practically no metal load have determined the transformation and mineralization of volcanic glass (the bentonitization–Na-smectitization process) and the deposition of silica varieties (“quartzine”, “chalcedonite”, opal-C), celestine and barite *etc.* along fissures–fractures and in the pore and lithophyse system.

5.1. BENTONITIC (Na-SMECTITIC) ARGILLIZATION

The bentonitic argillization was the transformation process that affected the entire volcanoclastic body from Valea Chioarului originally constituted of vitroclastic tuff and vitrophyric rhyolite. Nevertheless, the process registered various intensities in different areas, as suggested by the heterogeneous transformation degree of the rock. Bentonitization was less significant in the northern extremity of the structure; there, the primary rock is a porous, cristobalite-rich vitroclastic tuff. In the middle part, the core of the body – as identified in underground mining works (panels 4, 9, 10, 10A, 12B *etc.*), was argillized only locally. This resulted in the formation of cm-wide nests that imprint to the rock a brecciated, spotted aspect. The source of the argillization process must have been related to epithermal solutions. They were acting during the final stage of the consolidation, *i.e.*, the **phreatic eruption** characterized by thermalized aqueous solutions.

Macroscopy. The bentonite is a compact rock, displaying various colours: white; white with greenish spots due to local chlorite concentrations; light grey (in most of the cases), sometimes with light greenish fissures that fade when the rock undergoes dehydration, turning into light grey colour. The rock is frequently breccified and tectonized, with distinct friction planes coloured in grey-red hues due to the infiltration of iron hydroxides. The rock includes numerous sedimentary elements (3–4 cm Ø), mainly rounded quartzite clasts, fragments of sandstones and sandy clay. Some samples contain silica micro- (1–3 mm Ø) and macro-nodules (1–4 cm Ø) that can reach up to 25 % of the bentonite mass. These nodules are irregular in shape, and display a rough surface. They consist of celestine partly replaced by silica, and of barite totally replaced by celestine and silica. Barite can be recognized based on its typical tabular crystalline habit, replaced in a first stage by celestine, and then by silica.

Microscopy. Based on microscopic features such as microlamellar, feathery texture built-up by a smectitic mass preserving the original features, we estimate that the primary rock for this bentonite was represented by vitroclastic tuff. The original fabric of the tuff is outlined by typical X-like, Y-like, globular or complex-shaped vitroclasts, with fragments of fibrous glass, all affected by argillization (Fig. 10). In lithophyses we noticed fibro-radial “quartzine” and in the vesicular voids, clay minerals; sometimes chalcedony represents the core, and clay minerals form a rim in the empty spaces. The concentrations of relic minerals consist of: quartz (1.5–6 %), sanidine (0.2–11 %), plagioclase (0.8–10 %),

⁵ Analysis carried out by the geologist I. Pintea.

and biotite (0.2–0.35 %) with microlites of zircon and apatite (Figs. 11–13). The clasts of sedimentary rocks are made of sericitic quartzite (these clasts are 0.80–1.00 mm in size) and of quartz xenocrysts with undulatory extinction, representing 1–2 % of the rock. The supergene impregnation of the bentonite with Fe-hydroxides confers a reddish tint to the whole rock. It is worthy to mention the seldom presence of some andesite fragments (0.25×0.30 – 0.70×0.80 mm in size) with porphyric texture (Fig. 14), characterized by the presence of two generations of feldspars (0.01×0.04 mm, and respectively 0.04×0.20 mm in size), biotite transformed into Fe-hydroxides (0.07×0.10 mm) and magnetite microcrystals in the matrix. The rock is similar to the andesite occurring in Pomăt Hill, Moigrad. Very rarely, we have identified angular fragments (0.38×0.45 mm) of hyalopilitic andesite with oriented texture. Marginally, these display signs of feeble magmatic corrosion; the vitrified corroded rim was argillized. The andesitic fragments represent enclaves in the rhyolite, originating from a deeper-rooted magmatic structure.

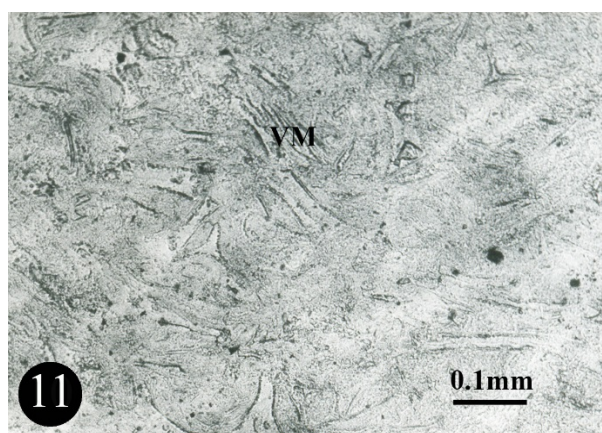


Fig. 11 – Bentonite formed on vitroclastic tuff (sample 2). 1N.

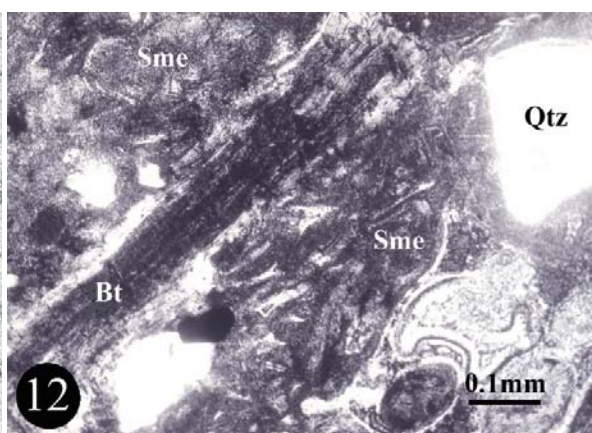


Fig. 12 – Bentonitized vitroclastic tuff (Sme). Quartz (Qtz) and partly argillized biotite (Bt) (sample 7). 1N.

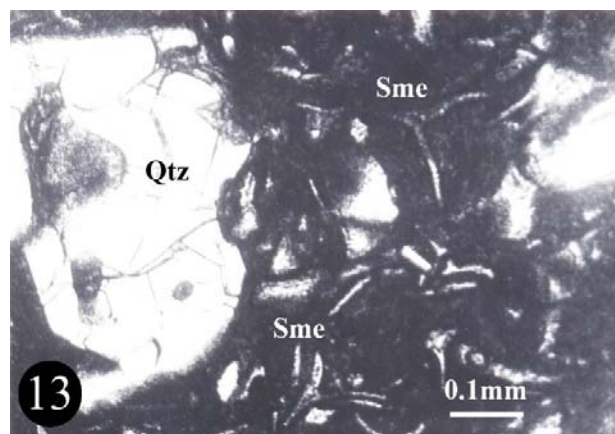


Fig. 13 – Bentonitized vitroclastic tuff (Sme). Quartz (Qtz) and partly argillized biotite (Bt) (sample 7). 1N.

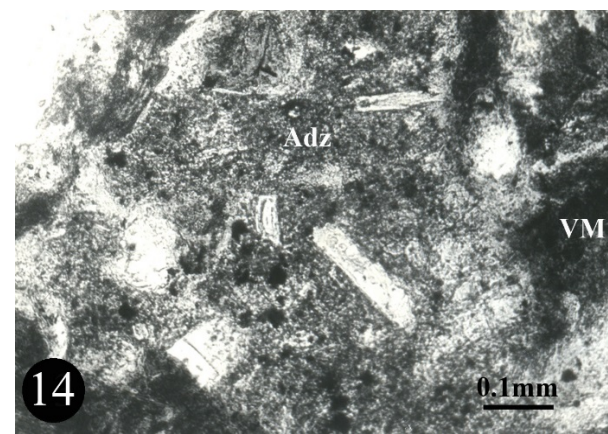


Fig. 14 – Microenclave of hyalopilitic andesite in bentonite (sample 1). 1N.

Under the microscope, the silica nodules consist of fibro-radial „quartzine” (Fig. 15) associated with celestine and barite. The latter two minerals were formed at the same time, thus often they occur as inclusions of one into the other. The silica deposition was a relatively long-lasting process, thus it partly replaced both previously formed minerals.



Fig. 15 – Fibro-radial quartz (“quartzine”) partly substituting barite (Brt) and celestine (Cls). N+.

The quartz–celestine association was also evidenced in the X-ray patterns of the celestine crystals collected from fissures and nodules (Table 4).

Table 4

Mineral assemblage based on XRD pattern (sample 14)

XRD parameters		Minerals	
<i>d</i>	<i>I</i>	<i>Celestine</i>	<i>Quartz</i>
4.266	12		+
3.439	100	+	
3.343	90		+
3.297	20	+	
3.183	10	+	
3.101	4	+	
2.976	10	+	
2.739	6	+	
2.451	5		+
2.280	6		+
2.144	8	+	
2.047	6	+	
2.004	6	+	
1.819	6		+

6. MINERALOGY OF THE CLAY FRACTION

Eight samples (no. 1, 2, 4, 5, 7, 8, 13 and 14) collected from underground mining works were used for evaluating the mineralogical composition of the clay fraction and the degree of bentonitization of the mineral assemblage. We have investigated two clay fractions, separated quantitatively: <5 μm and <2 μm .

6.1. CLAY FRACTION <5 μm

The amount of clay minerals separated by using the sedimentation-siphoning method varied in each individual sample. The highest content was noticed in samples 1, 2 and 4 (69–79 %), while the lowest one in samples 13 and 14 (19–31 %). In the rest of the samples, the clay fraction represented ~50 % of the whole rock mass (Table 5).

Table 5

Quantitative distribution of the clay fraction (<5 μm) in the studied samples

Sample no.	Clay fraction (%)	Residue (%)
1	76	24
2	79	21
4	69	31
5	53	47
7	45	55
8	57	43
13	31	69
14	19	81

Clay minerals are almost absent in the residue obtained after the separation of the <5 μm fraction; instead, its mineral spectrum is represented by quartz, feldspars and biotite, rare fragments of sedimentary rocks, relicts from the argillized rock, and nodular silica.

The clay fraction is dominated by sodium- rich smectite. Additionally, partly or fully hydrated mica lamellae, illite, various amounts of silica, accidentally kaolinite and totally subordinate halloysite were also identified.

6.2. CLAY FRACTION <2 μm

Na-rich smectites represent the main minerals of the <2 μm fraction in all the investigated samples. Besides, the mineral association includes micas, illite, illite/montmorillonite, kaolinite, cristobalite, amorphous silica and totally subordinately, halloysite.

The specific crystallographic and morphological features of the minerals in the clay fraction are of utmost importance when deciphering the argillization process, *i.e.* mainly represented by smectitization, as well as the potential subsequent mechanical and/or chemical alterations they have undergone. Electron microscopy is the best method to provide such information. The results of our TEM and SEM investigations on the most representative samples are presented below.

6.2.1. TEM study

For this study, we have selected four samples collected from representative locations in the bentonite ore: near the contact with the Paleogene hanging wall (sample 1); in the Cretaceous bedrock (sample 14); and in the core of the bentonitized body (samples 2 and 5).

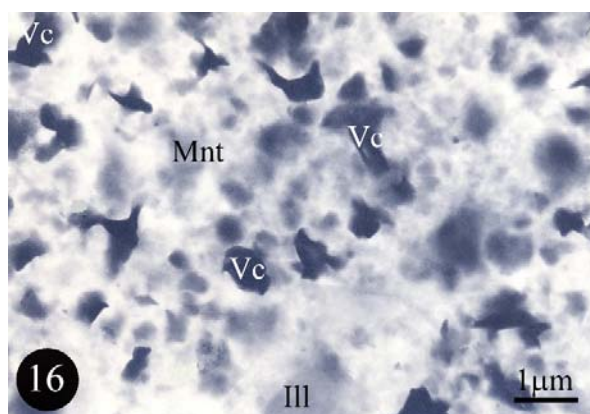


Fig. 16 – TEM. Montmorillonite (Mnt) as finely grained xenomorphous aggregates with hairy morphology, illite (Ill) and fresh, or partly argillized vitroclasts (Vc) (sample 1).

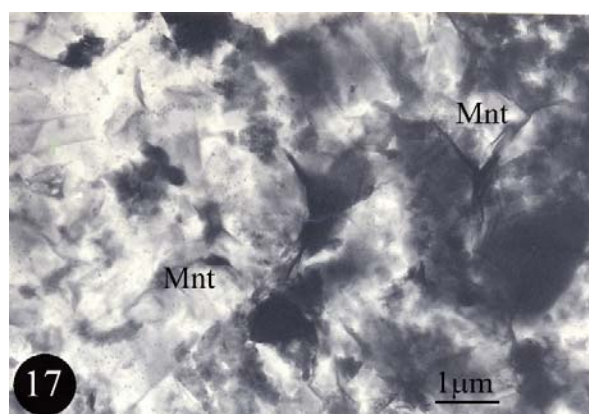


Fig. 17 – TEM. Two generations of montmorillonite (Mnt): large lamellae (in most of the sample) and small lamellar aggregates (sample 2).

The clay fraction of sample 1 (Fig. 16) is dominated by degraded montmorillonite, present as fine, feather-like aggregates; individual lamellae could not be identified. The clay matrix contains relatively large concentrations of small, fresh or partly argillized fragments of volcanic glass (Fig. 16) and totally subordinate xenomorphous lamellae of illite (probably from the clay in the top layer).

Sample 2, collected from the same level as sample 1 but located towards the centre of the bentonitized body, displays a totally different range of crystal sizes. The TEM image illustrates two generations of crystals: a) evenly thick large lamellae with irregularly bent or twisted rims; and b) smaller crystals with various thicknesses that do not expose signs of alteration (Fig. 17). As a rule, the surface of the lamellae is covered with grey spherules (<0.1 μm \varnothing) of amorphous silica. The large smectite lamellae are accompanied by prismatic illite/montmorillonite crystallites and, basically xenomorphous illite; rarely, fresh volcanic glass was also detected.

In sample 5, smectite is present as unevenly twisted, well-crystallized lamellae with indistinct rims (Fig. 18). In subordinate amounts, we have identified xenomorphous mica (probably biotite, given the tiny separations of opaque minerals noticeable under the electron beam) lamellae with ragged and thinned rims as a result of the alteration processes, *i.e.*, illitization and montmorillonitization. The fine powdery cristobalite is evenly distributed in the clay matrix.

The clay fraction in sample 14 (Fig. 19) consists of a mixture of larger lamellae with heterogeneous thickness and twisted rims, and frequent lamellar fragments associated with fine feathery degraded montmorillonite aggregates. The montmorillonite matrix contains partly argillized fragments of volcanic glass, rare xenomorphous lamellae of partly hydrated mica, and seldom goethite and amorphous silica.

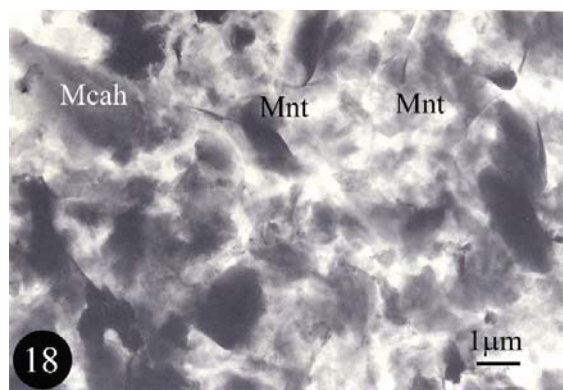


Fig. 18 – TEM. Montmorillonite (Mnt) as xenomorphous lamellar aggregates, and partly hydrated micas (Mcah) (sample 5).

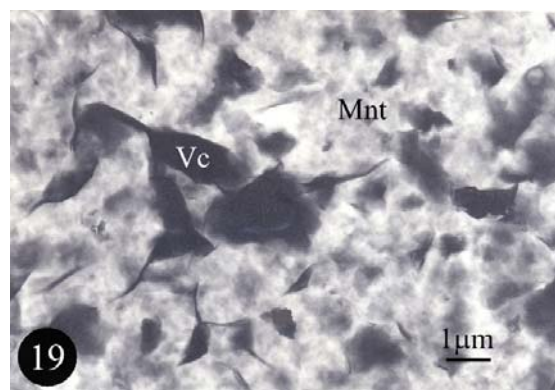


Fig. 19 – TEM. Montmorillonite (Mnt) as xenomorphous lamellar aggregates and vitroclasts (Vc) (sample 14).

6.2.2. SEM study

The SEM images, due to the three-dimensional perspective on broken surfaces, are more conclusive in understanding the details of the argillization processes. More than that, the samples included in the SEM study were carefully selected based on their location in the deposit, in order to provide meaningful insight into the stages of smectitic transformation of the bentonitized rock. The six selected samples can be grouped according to distinct fabric types displayed, as follows: type 1 – samples 2, 4; type 2 – samples 5, 7, 23; and type 3 – sample 8.

For investigating sample 2, we have used the same area illustrated in the TEM image that illustrates the two types of aggregates (see above). Additional to the previous information, in the SEM image (Fig. 17), we could observe cristobalite crystals in the finely-crystallized montmorillonite matrix. The presence of the two generations of crystals of montmorillonite is more obvious in sample 4 (Fig. 20).

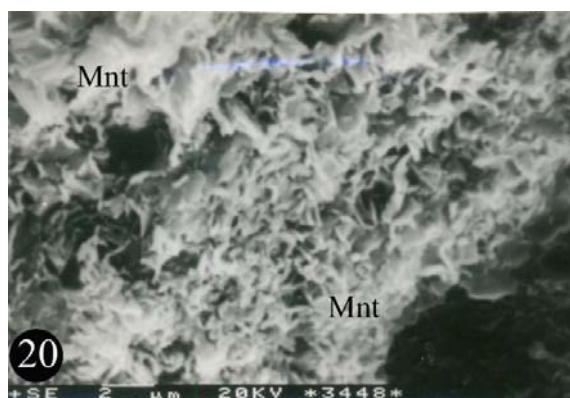


Fig. 20 – SEM: Two generations of crystallized Na-montmorillonite (Mnt) (sample 4).

The lamellae of the first generation, even if not abundant, sometimes exceed 5 μm in size; one cannot exclude the idea that mica was their precursor. The groundmass consists of an aggregate of fine ($\sim 1 \mu\text{m}$) bent lamellae with twisted rims. The small cristobalite crystals, more abundant than in sample 2, form small aggregates in the montmorillonite matrix.

Samples 5 and 7 show common SEM features represented by vermicular structures that are not typical in the rest of the samples (Figs. 21, 22). The vermicular fabric consists of bordering crystal planes in-between which single (Fig. 21) or double (Fig. 22) vermicular aggregates developed. The montmorillonite lamellae line-up perpendicular to the bordering planes; sometimes parallel overgrowths were noticed, marked by the reiteration of two rims intersecting at 120° . Cristobalite was not identified within the vermicular areas, but it forms concentrates on the surface of the bordering planes. Vermicular fabric was also identified in sample 23. Most of the Na-montmorillonite lamellae are relatively large and of homogeneous thicknesses; they are slightly bent, and show unevenly twisted rims. We have also observed rare aggregates consisting of small lamellae.

The SEM image of sample 8 (Figs. 23, 24) also evidences the presence of the two generations of crystals. The larger ones are dominant, consisting of undulated, mainly xenomorphous lamellae with homogeneous thicknesses; they sometimes display ragged ends (probably due to overgrowths) and unevenly twisted rims. The display of the Na-rich smectite lamellae suggests that they have replaced fibrous vitroclasts. In-between the lamellae with ragged ends, we have noticed aggregates of smaller, idiomorphous crystals with systematic display. Cristobalite forms small, tabular crystals and it is mainly located on some of the ragged lamellae.



Fig. 21 – SEM: Vermicular structures of Na-smectite (Mnt) (sample 5).



Fig. 22 – SEM: Vermicular structures of Na-smectite (Mnt) and cristobalite (Crs) (sample 7).

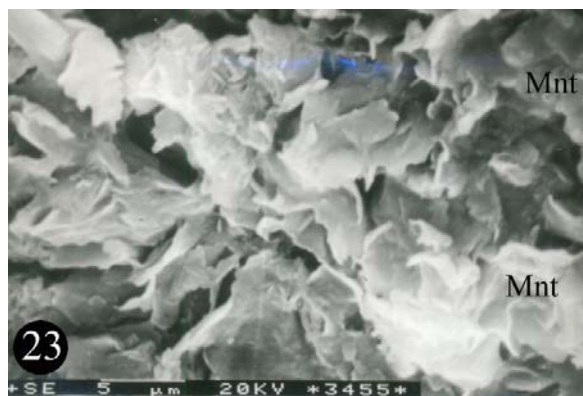


Fig. 23 – SEM: Na-smectite with fringed ends (Mnt).
(sample 8).

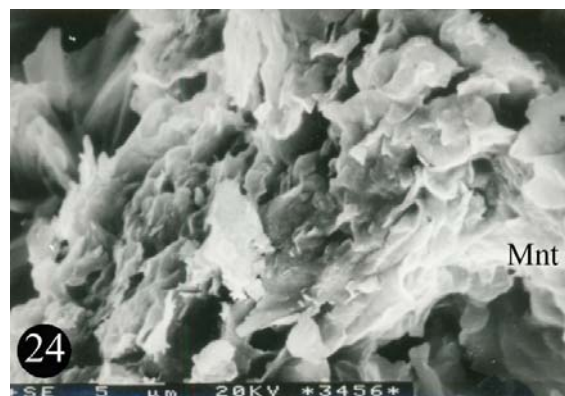


Fig. 24 – SEM: Na-smectite with fringed ends (Mnt).
(sample 8).

6.2.3. Genetic considerations on the smectitized rocks

Based on the fabric of the products of montmorillonitic transformations, as illustrated by the SEM images, we have defined the following groups of samples: 1) displaying two generations of crystals differing in their crystallinity degree (samples 2, 4 – vitroclastic tuffs); 2) consisting of montmorillonite with vermicular fabric, where the lamellae developed perpendicular to the two bordering planes (samples 5, 7, 23 – vitrophyric rhyolite); 3) with lamellar crystals showing rugged ends (sample 8 – fibrous vitroclasts originating from vitroclastic tuffs); and 4) with degraded montmorillonite (samples 1, 14 – located close to the surface and to the contact with sedimentary rocks).

6.2.4. Cristobalite

The Na-rich smectite from the Valea Chioarului bentonite ore is accompanied by cristobalite resulted from the transformation of glass into smectite. As a rule, cristobalite lines the voids in the rock, being present as globular or, in the case of planar backgrounds, layered aggregates. The individual crystals are tabular, and they cross each other under 90° and 45° angles, based on their tetragonal symmetry (Fig. 25).

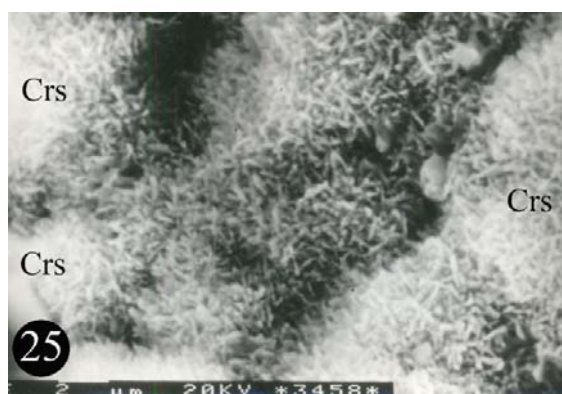


Fig. 25 – SEM: Cristobalite (Crs).

6.2.5. X-ray diffraction

The identification of the clay minerals in the clay fraction by the means of X-ray diffraction (XRD) is based on their individual crystal structures (in raw and oriented samples), and their behaviour when treated with ethylene glycol, or heated at various temperatures (350° C, 500° C, or 1000° C). The changes affecting the distance between the basal planes (00 ℓ) when samples are treated

with ethylene glycol as compared to that in the untreated sample prove the typical expandability of the smectitic and mixed-layered structures.

The XRD pattern of sample 1 (clay fraction $<5 \mu\text{m}$, oriented sample) illustrates a reduced number of relatively wide bands, as a sign of the reduced crystallinity degree of the mineral phases. The most intense lines correspond to Na-montmorillonite as dominant phase. Additionally, in small amounts as indicated by the feeble intensity of the corresponding lines, we have identified illite ($d=10.39 \text{ \AA}$, $I=4$; $d=3.32 \text{ \AA}$, $I=4$), kaolinite ($d=3.58 \text{ \AA}$, $I=6$) and cristobalite ($d=4.06 \text{ \AA}$, $I=10$). When comparing the XRD patterns of the two clay fractions ($<5 \mu\text{m}$ vs. $<2 \mu\text{m}$) in sample 1, we noticed a lower cristobalite content in the coarser one. All the non-treated oriented samples of the clay fraction $<2 \mu\text{m}$ obtained from the 8 studied bentonites reveal the typical lines of Na-montmorillonite, corresponding to (00ℓ) planes: 12.4 (001), 6.2 (002), 4.07 (003), 3.14 (004), or to $(0k0)$ planes: 4.47 (020) and 1.49 (060) (the numbers as in sample 5, Fig. 26, and the planar distances expressed in \AA). The (00ℓ) planar distances recorded in the samples treated with ethylene glycol are higher: 17.11 (001), 8.49 (002), 5.64 (003), 4.22 (004), 3.37 (005) and respectively 2.81 (008) (Fig. 26). The basal distance for the (001) plane, and the migration of the (00ℓ) band towards higher values following glycolation are clear arguments for assigning this clay phase to Na-montmorillonite.

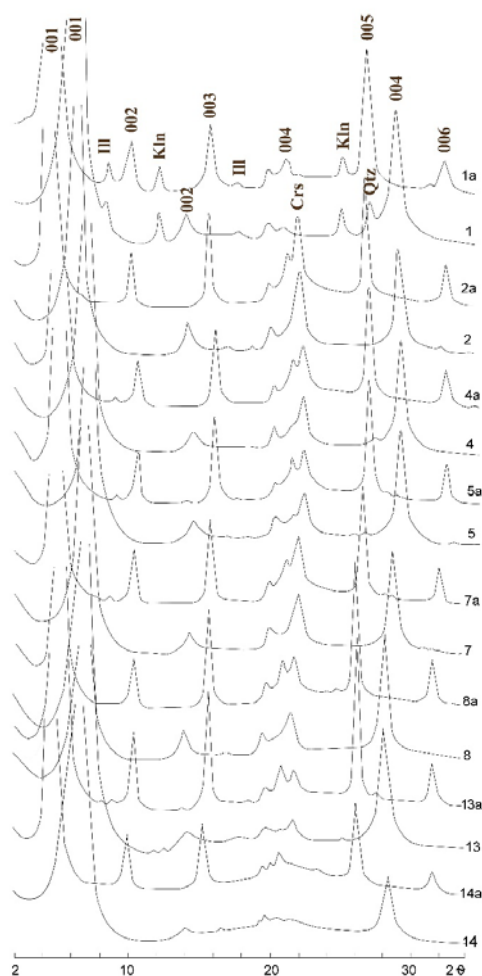


Fig. 26 – X-ray diffraction patterns of the $<2 \mu\text{m}$ clay fraction. Oriented samples: 1, 2 etc.; oriented samples with ethylene glycol: 1a, 2a etc.

Besides the main clay mineral (Na-montmorillonite) representing ~ 90 % of the mass of this clay fraction, we have identified the following minerals, in decreasing order of frequency: cristobalite ($d=4.03\text{--}4.05\text{ \AA}$) in all the studied samples, illite and partly hydrated mica; quartz is totally subordinate ($d=3.34\text{ \AA}$). The XRD pattern of sample 1 shows two bands (7.1 \AA and 3.58 \AA) corresponding to a non-expandable mineral, which we assign to kaolinite-*d* (Fig. 26). Table 6 synthesizes the quantitative mineral composition of the eight studied clay fractions, calculated based on proportional ratios.

Table 6

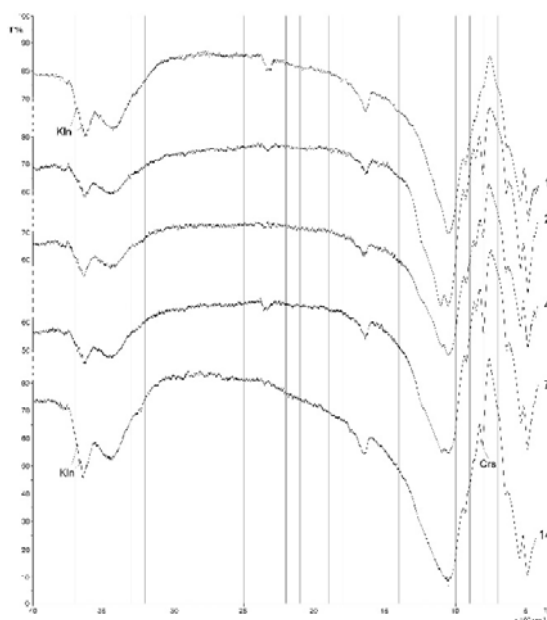
Quantitative mineralogical composition (%) of the $<2\text{ }\mu\text{m}$ clay fraction #

Mineral	Sample 1	Sample 2	Sample 4	Sample 5	Sample 7	Sample 8	Sample 13	Sample 14
Montmorillonite	88.5	87	88	91	87	91	95	99
Illite	4	-	-	-	1.5	-	-	-
Kaolinite	4	-	-	-	-	-	-	-
Cristobalite	0.5	13	11.5	9	11.5	9	5	1
Quartz	3	-	0.5	-	-	-	-	-

6.2.6. IR spectroscopy

Vibrational infrared (IR) spectroscopy provides data on the molecular structure of the minerals in the clay fraction, by evidencing the atomic groups and the molecules in their crystal structure.

When compared with the standard montmorillonite spectrum, the IR spectra of the clay fractions in the five investigated samples (Fig. 27) prove the presence of montmorillonite. Samples 1 and 14 are almost identical with the reference spectrum, thus monomineralic; we consider them as being composed of degraded montmorillonite. The typical IR adsorption bands of montmorillonite are the effect of the presence of water, and respectively of OH: 1645 cm^{-1} is the water band, while 3450 cm^{-1} in sample 14, or 3420 cm^{-1} in sample 1, and respectively $3630\text{--}3640\text{ cm}^{-1}$ are two bands corresponding to the two OH positions. However, as compared to the standard spectrum, we noticed two differences in the $400\text{--}1200\text{ cm}^{-1}$ interval. The first one concerns the adsorption band at 470 cm^{-1} that migrates to $490\text{--}495\text{ cm}^{-1}$; this migration may be caused by substitutions of Si with Al^{+3} and Fe^{+3} in the tetrahedral layer.

Fig. 27 – IR spectra on the clay fraction $<2\text{ }\mu\text{m}$.

The second difference is related to the main adsorption band, the one representing the Si–O–Si bond. In the case of samples 1 and 14, this band shows a single peak, at 1050 cm⁻¹ (sample 1) and respectively 1060 cm⁻¹ (sample 14). The other three samples show two neighbouring peaks: the first one at values similar to the previously mentioned ones, and the second one in the 1105–1120 cm⁻¹ interval. We associate the second peak with increased expandable layers content.

Based on the IR spectra, we conclude that the clay fraction is dominated by two smectitic phases, as already suggested by the morphological-crystallographic features evidenced by electron microscopy (TEM and SEM): one twisted, finely-lamellar, with heterogeneous thicknesses; and one largely crystallized, with homogeneous, undulated or unevenly bent lamellae. We assign the two phases to Na-montmorillonite and respectively Na-beidellite, the latter probably originating from micas.

Additionally, the IR spectra indicate two other types of minerals mixed with smectite: cristobalite, identified in all the samples (rare in sample 1, and more frequent in samples 4 and 2) and kaolinite (samples 1 and 14) – the latter evidenced by the bands at 3656 cm⁻¹ and 3696 cm⁻¹.

6.2.7. Chemistry

The path taken by the geochemical transformations during the bentonitization process, in terms of chemical elements supplied *vs.* the ones removed, is illustrated by the changes in the chemistry of the primary rock, as compared to the raw bentonite and its clay fraction (Table 7).

Table 7

Chemical transformations during the smectitization process

Oxides	Rhyolite (fragments) (Untului Brook)	Raw montmorillonitic bentonite (grey)	Montmorillonitic bentonite, clay fraction <1 μm
SiO ₂	77.10	64.42	63.74
TiO ₂	0.19	0.19	0.20
Al ₂ O ₃	11.34	13.02	14.77
Fe ₂ O ₃	0.88	1.48	1.22
FeO	0.26	0.35	0.60
MnO	0.019	0.02	0.02
MgO	1.36	3.22	4.06
CaO	0.70	0.63	0.89
K ₂ O	5.80	0.70	0.16
Na ₂ O	0.75	0.88	0.87
P ₂ O ₅	0.10	0.062	0.022
H ₂ O ⁺	0.95	3.44	5.04
H ₂ O ⁻	0.58	11.70	9.05
Total	100.029	100.112	100.642

The oxide composition of the three samples, *i.e.*, rhyolite, raw bentonite and its clay fraction, illustrates the path taken by the chemical transformations during the bentonitization process: a remarkable decrease of the SiO₂ content: from 77.10 % in the rhyolite, respectively 76.87 % in the porous, vitroclastic tuff, to 64.2 % in the raw bentonite, and 63.74 % in the montmorillonite-rich clay fraction <1 μm (Table 4). The same trend is recorded by the alkalies (K₂O+Na₂O): from 6.55 % in the rhyolite to 1.03 % in the clay fraction. The decrease in the alkalies content is accompanied by a dramatic change of the K₂O:Na₂O ratio from 8:1 to 1:1, resulting in the K-release and the preferential retention of Na, with the formation of the Na-montmorillonite.

The main feature of the investigated hydrothermal bentonitization process is represented by the leavitation of K from the rhyolitic rock and the parallel Na incorporation in the neoformed clay mineral. Under the influence of the hydrothermal solutions, K is depleted and leaves the system, probably as a silicatic phase; on the other hand, the source for Na may be represented, in the case of a phreatomagmatic eruption, by seawater.

Bentonitization took place under low temperature, and slightly alkaline hydrothermal conditions. The high porosity of the rock controlled and favoured the argillization process. Given the low metallic load of the hydrothermal solutions, metallic minerals are scarce; they are represented by pyrite, marcasite and hematite, associated with quartz in geodes or in the bentonitic mass. For example, we have identified hexahedral pyrite crystals up to 0.1 mm in size.

7. CONCLUSIONS

The present contribution focuses on the geology of Valea Chioarului bentonite and provides the most consistent analysis of the argillization process affecting the diverse primary rocks, *i.e.*, vitrophyric rhyolites and vitroclastic tuffs based on complex modern analytical methods.

The chemical analyses on samples of rhyolite, raw bentonite and montmorillonitic bentonite (<1 μm fraction) evidence the path taken by the chemical transformations during the bentonitization of the primary rock. The following trends were identified:

- a significant decrease of the SiO_2 content, from 77.10 % (rhyolite) or 76.87 % (vitroclastic tuff), to 64.20 % (raw bentonite) and 63.74 % in the montmorillonitic fraction (<1 μm);
- the decrease of the alkalis content ($\text{K}_2\text{O}+\text{Na}_2\text{O}$) follows a similar trend, from 6.55 % (rhyolite), to 1.03 % in the montmorillonitic fraction;
- a dramatic change in the alkalis composition: the $\text{K}_2\text{O}:\text{Na}_2\text{O}$ decreased from 8:1 to 1:1; this illustrates the levigation of K and the incorporation of Na, with the formation of Na-rich smectites. The K removal, probably *via* silicatic phase, took place through chemical exchange reactions, controlled by the hydrothermal solutions leading to argillization. Based on our results, we can state that bentonitization occurred as a result of the circulation of slightly alkaline epithermal solutions, depleted in metallic elements.

The smectitic minerals resulted in the bentonitization process show heterogeneous compositions. Our investigations evidenced the presence of Na-montmorillonite and Na-beidellite.

REFERENCES

- Cloos, H. (1969), *Dialogue with the Earth (in Romanian)*. Edit. Șt. București, 415 p.
- Grengg, R. (1920), *On the soapy Earth from Gaura in Transylvania (in German)*. Verhandl. Der Geol. Staatsanstalt, Jahrgang 1920. geologischen spezialaufnahmen. Földt. Közl., **XI**, 317–329.
- Grengg, R. (1940), *The soapy Earth from Gaura in Transylvania (in German)*. Tonindustrietzg, **LXIV**(61), 459–462; 62, 472–473.
- Ghergari, L., Ionescu, C. (2000), *Gem-quality materials associated with Laramian magmatites in the Valea Chioarului area, Transylvania (Romania)*. 31st International Geological Congress, Abstr. vol.,-CD, Rio de Janeiro, Brazil.
- Ghiurcă, V., Mârza, I. (1991), Note on a vitroclastic tuff bed (friable)-stratigraphic landmark in the Lower Badenian from the Baia Mare Basin. In: Mârza I. (ed.) *Geological Formations of Transylvania, Romania, 3. The Volcanic Tuffs from the Transylvanian Basin, Romania 1991*, Cluj-Napoca, 45–49.
- Hauer, F., Stache, G. (1863), *Geology of Transylvania (in German)*. W. Braumüller, Wien, 636 p.
- Hofmann, K., (1886), *Geological notes on the Preluka crystalline schists island and the connecting northwards and southwards Tertiary hills (in Hungarian)*. Magy. Kir. Földt. Int. Évi. Jelentése 1885-ről, Budapest, 27–51.
- Ioniță, S. (1964), *The Mesozoic and Paleogene in Vărai–Curtuiuş–Gaura–Valea Chioarului area (in Romanian)*. D.S., **L**(1), (1962–1963), 335–348.
- Kalmár, I., Ionescu, D. (1972), *On the andesitic agglomerates in the Upper Badenian deposits from Chioarului Gorges (in Romanian)*. St. cerc. geol.-geofiz.-geogr., geologie, **2**, 413–417.
- Kalmár, I. (1975), *Considerations on the geology and petrography of the rhyodacitic neck from Valea Chioarului (Maramureș County) (in Romanian)*. St. cerc. geol.-geofiz.-geogr., geologie, **20**, 187–202.

- Mărgărit, Gh., Mărgărit, M. (1968), *The horizons within the Paleogene deposits in Valea Chioarului area* (in Romanian). St. cerc. geol.-geofiz.-geogr., geologie, **14**, 253–260.
- Mârza, I., Ghergari, L. (1963), *The bentonite from Valea Chioarului (Maramureș County). (Preliminary note)* (in Romanian). Rev. Min., **1**, 41–43.
- Mârza, I., Ghergari, L. (1967), *The geological and mineralogical study of the bentonite from Valea Chioarului (Maramureș region)* (in Romanian). Anal. Univ. București, Ser. Șt. Nat., Geol., Geogr., **XIV**(1), 31–45.
- Popescu, B. (1978), *On the lithostratigraphic nomenclature of the NW Transylvania Eocene*, Revue Roum. Géol.- Géophys.- Géogr., Géologie, **22**, 99–107, București.
- Popescu, B. (1984), *Lithostratigraphy of cyclic continental to marine Eocene deposits in the NW Transylvania, Romania*, Archives Scientifiques Genève, **37**(1), 37–73, Geneva.
- Szentés, F. (1950), *About the bentonite from Gaura, northern Transylvania* (in Hungarian). A Magyar Állami Földt. Intézet Évi Jelentése, 1943, II Kötet, Budapest, p. 393.
- Ștefan, A., Rusu, A., Bratosin, I. & Colios, E. (1986), *Petrological Study of the Alpine Magmatites in the Link Zone between the Apuseni Mountains and the Oaș–Gutâi–Țibleș Volcanic Chain*. D. S. Inst. Geol. Geofiz., **70–71**(1), (1983–1984), 243–262.
- Ștefan, A., Lazăr, C., Berbelec, I. & Udubașa, Gh. (1988), *Evolution of Banatitic Magmatism in the Apuseni Mts. and Associated metallogenesis*. D. S. Inst. Geol. Geofiz., **72–73**(2), (1985–1986), 195–213.